3D-Printed models for left atrial appendage occlusion planning: a detailed workflow

Tommaso Stomaci and Francesco Buonamici
Department of Industrial Engineering, Università degli Studi di Firenze, Florence, Italy
Giacomo Gelati and Francesco Meucci
Department of Clinical and Experimental Medicine, Structural Interventional Cardiology, Azienda Ospedaliero Universitaria Careggi, Firenze, Italy, and
Monica Carfagni
Department of Industrial Engineering, Università degli Studi di Firenze, Florence, Italy

Abstract

Purpose – Left atrial appendage occlusion (LAAO) is a structural interventional cardiology procedure that offers several possibilities for the application of additive manufacturing technologies. The literature shows a growing interest in the use of 3D-printed models for LAAO procedure planning and occlusion device choice. This study aims to describe a full workflow to create a 3D-printed LAA model for LAAO procedure planning.

Design/methodology/approach – The workflow starts with the patient's computed tomography diagnostic image selection. Segmentation in a commercial software provides initial geometrical models in standard tessellation language (STL) format that are then preprocessed for print in dedicated software. Models are printed using a commercial stereolithography machine and postprocessing is performed.

Findings – Models produced with the described workflow have been used at the Careggi Hospital of Florence as LAAO auxiliary planning tool in 10 cases of interest, demonstrating a good correlation with state-of-the-art software for device selection and improving the surgeon's understanding of patient anatomy and device positioning.

Originality/value – 3D-printed models for the LAAO planning are already described in the literature. The novelty of the article lies in the detailed description of a robust workflow for the creation of these models. The robustness of the method is demonstrated by the coherent results obtained for the 10 different cases studied.

Keywords Left atrial appendage occlusion, Structural heart surgery, 3D Printing, Stereolithography, Surgical planning, Heart model, Additive manufacturing, Left atrium

Paper type Research paper

Plain language summary

Atrial fibrillation is common in elderly people, and one of its most critical consequences is an increase in stroke risk due to thrombi formation in the left atrial appendage (LAA). Left atrial appendage occlusion (LAAO) is one of the surgical interventions used to reduce this risk. The intervention, performed via catheter, consists in the installation of a plug device in the neck of the LAA, preventing thrombi from leaving it. Given the great anatomical variability of the LAA, the correct sizing and individuation of the device placement might result challenging if based only on diagnostic images. 3 D printing technologies can provide support in the intervention planning phase with patient-specific appendage models, useful for three-dimensional visualization of the appendage and for supporting the device selection. In this article, a workflow for the creation of these models is described, starting from standard diagnostic images used for procedure planning and ending with patient-specific flexible 3 D-printed models which can be used by physicians to support the intervention decision-making process.

1. Introduction

Atrial fibrillation is the most common cardiac arrhythmia, affecting a consistent percentage of the over 80 population of the elderly population (Krijthe *et al.*, 2013; Piccini *et al.*, 2012; Ryder and Benjamin, 1999; Wilke *et al.*, 2013).

The current issue and full text archive of this journal is available on Emerald Insight at: **https://www.emerald.com/insight/1355-2546.htm**

Rapid Prototyping Journal
29/11 (2023) 74–81
Emerald Publishing Limited [ISSN 1355-2546]
[DOI 10.1108/RPJ-10-2022-0351]

The study described in the present paper was carried out within the "Custom3D – Customized 3D in medicine" Laboratory, a joint lab between the Department of Industrial Engineering of Florence and the Careggi Hospital of Florence. No external funding was received.

Received 13 October 2022
Revised 13 February 2023
2 May 2023
Accepted 4 May 2023

Atrial fibrillation is associated with a fivefold increase in ischemic stroke risk; up to 20% of all ischemic strokes can be reconducted to an atrial fibrillation condition (Beigel *et al.*, 2014; Benjamin *et al.*, 1998; Furberg *et al.*, 1994; Kodani and Akao, 2020; Lee *et al.*, 2018). Left atrial appendage (LAA) has been identified by several studies as the principal thrombi formation location (Al-Saady *et al.*, 1999; Nucifora *et al.*, 2011; Stoddard *et al.*, 1995).

The LAA is a long, tubular, ear-shaped pouch connected with the atrium main chamber through a narrow connection. High anatomic variability characterizes the shape of the LAA; four principal families of LAA shapes are described in the medical literature: cactus, chicken wing, cauliflower and windsock (Figure 1). Nevertheless, LAA shapes are often difficult to categorize within rigid boundaries, and even the dimension of the LAA anatomy seems heavily dependent on patient characteristics (Beigel *et al.*, 2014). Finally, patient-specific micro features are always found in each case, as the internal LAA structure is not smooth, but intricated and defined by the presence of a series of muscles (pectinate muscles) that line the cavity of the appendage (Su *et al.*, 2008). The intricated morphology of the LAA predisposes it to blood stasis and endothelial dysfunction, resulting in the up mentioned cardiac thromboembolism formation risk (di Biase *et al.*, 2012).

Pharmacological treatment with oral anticoagulation therapy can reduce the thromboembolic risk, but for patients who cannot undergo prolonged pharmacological therapy surgical treatment can be suggested (Hindricks *et al.*, 2021). Percutaneous left atrial appendage occlusion (LAAO) is the main mechanical prevention measure against left atrial thromboembolism (de Backer *et al.*, 2014; Blackshear and Odell, 1996). With respect to open-chest interventions like LAA excision or clipping, percutaneous LAAO is less invasive, which is a clear advantage for elderly, fragile patients (Caliskan *et al.*, 2017).

In a percutaneous LAAO procedure, a delivery catheter is inserted in the femoral vein, then advanced into the inferior vena cava up to the patient's heart right atrium. Trans-septal puncture is performed in the fossa ovalis to gain access to the left atrium, then the catheter is pushed towards the LAA, where a self-expanding occlusion device is finally delivered to seal the LAA orifice. The percutaneous intervention is navigated in real-time, to monitor the position of the catheter and the placement of the device, thanks to transesophageal echocardiography and angiography.

Plug umbrella-shaped occlusion devices are designed to prevent thrombi from leaving the LAA, by excluding it from the circulatory system through ostium obstruction. Device sealing and endocardialization, both affected by the correct placement in the landing zone, are needed for the correct functioning of the device. Different sizes and models are available on the market; in particular, Amplatzer Amulet (Abbott Vascular, Santa Clara, CA), available in lobe diameters from 16 mm to 34 mm, and Watchmen FLX (Boston Scientific, Marlborough, MA), available in diameters from 21 mm to 35 mm, are among the most used plug occlusion devices (Figure 2).

The main criticalities of the LAAO procedure are the selection and sizing of the occluding device, the choice of the landing zone (i.e. the area where the device is fixed in the LAA) and device positioning (Aminian *et al.*, 2018; Sawaya *et al.*, 2017; Unsworth *et al.*, 2011), which are all based on the patient diagnostic imaging from computed tomography (CT), trans-thoracic echography, trans-esophageal echography and magnetic resonance imaging (Wang *et al.*, 2010).

The previously described anatomical variability and complexity of the LAA result in significant uncertainty in the occluding device sizing and landing zone determination. Whenever the surgeon makes exclusive usage of diagnostic 3 D images, an average of 1.38 devices are used during each LAAO procedure due to incorrect sizing (Reddy *et al.*, 2017). Direct consequences of device mismatch are an increase in intervention complexity, an increase in intervention cost due to a greater number of devices required, an increased possibility of

Figure 1 Examples of left atrial appendage shapes

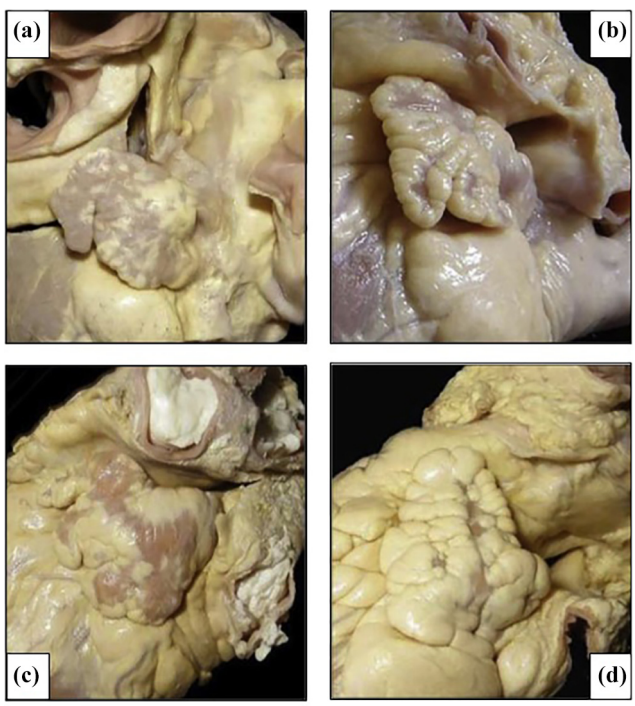

Notes: (a) Chicken wing; (b) cauliflower; (c) windsock; (d) cactus
Source: Beigel *et al.* (2014), courtesy of the authors

Figure 2 LAAO devices

Notes: Left: Amplatzer Amulet; right: Watchmen FLX
Source: Figure by authors

negative intervention outcome due to poor device fixation and blood leaking from the LAA.

The benefits of a combined multi-modal imaging and 3 D printing approach to the LAAO procedure planning are widely highlighted in the literature (Conti *et al.*, 2019; Graf *et al.*, 2014; Iriart *et al.*, 2018; Obasare *et al.*, 2018; Otton *et al.*, 2015); in particular, the possibility to rapidly create a tangible model of the LAA anatomy with flexible materials directly from the specific patient anatomy, with no need for specific and expensive molds to support the choice of LAAO device and determination of the landing zone is highlighted (Hachulla *et al.*, 2019).

This article describes a detailed workflow to obtain a 3 D-printed flexible model of the LAA, starting with the patient CT medical images to the print postprocessing procedures. The goal of the authors is hence to provide the reader with a robust approach for the production of flexible models of the LAA, minimizing the time resources required to complete the entire process, as the time window between the CT acquisition and the date of the intervention is usually limited.

The procedure has been used in 10 different clinical cases as a support to the surgeon's decision-making process. The cases were provided thanks to the collaboration with the Structural Interventional Cardiology Unit of the Careggi Hospital of Florence, which is a partner in the present study. The number of cases was deemed sufficient to address the variability of the LAA anatomy discussed earlier.

2. Material and methods

In addition to the diagnostic image acquisition, the workflow is composed of three principal steps: image segmentation, 3 D modeling and 3 D printing. The segmentation step consists in isolating the shape of the LAA from the diagnostic images and creating a 3 D geometrical representation of the anatomical structures. The 3 D modeling phase consists in a refinement of the geometry produced during the segmentation phase. The main scope of the 3 D Modeling phase is to ensure that the outcome of the workflow is manufacturable using the 3 D printing technology of choice; indeed, direct printing from segmentation phase does not usually produce models of the required quality. Finally, the 3 D printing process creates a physical simulacrum of the digital image through additive manufacturing (AM) technologies. Print cleaning and postprocessing are addressed in this phase.

Different additive manufacturing technologies and materials were analyzed to identify which provided the best response to the medical equip requests of model flexibility, transparency and cost efficiency in a preliminary phase of the activity. Polyjet technology (Stratasys, Eden Prairie, MN) and FormLabs (FormLabs; Somerville, MA) Stereolithography (SLA) were considered the most promising among all other processes.

SLA is an AM process exploiting the photopolymerization of specific liquid resins under a light source. The material, contained in a tank, is selectively exposed to a laser that triggers the solidification reaction; the path drawn by the laser spot on the liquid resin determines the shape of each layer. The movement of the building platform along the machine vertical (Z) axis guarantees the creation of contiguous layers, as a new layer of liquid resin is exposed to the laser. Material Jetting, of which Polyjet is one of the most diffused commercial application, produces solid parts exploiting the principles of inkjet paper printers, depositing micro drops of curable resin in the desired position across a layer and then curing them thanks to the exposition of a light source. The relative motion between the build platform and the printing head, on the z axis, allows for the deposition of a new layer of drops on the substrate.

Specimens of different Polyjet Cardiac materials were printed with a J850 Digital Anatomy Printer and compared with FormLabs Form 3+ Printer Elastic 50 A specimen. The medical equip judgment was in favor of SLA; flexibility and haptic response were considered similar for the two different technologies, but SLA prints demonstrated superior transparency and an inferior cost.

2.1 Diagnostic image acquisition

The workflow is designed to start from routine preinterventional diagnostic images so the default Careggi hospital procedure can be used for data acquisition, which has been derived from literature (Korsholm *et al.*, 2020). Patients' cardiac CT images are acquired using contrast for the blood pool of the left atrium and gating is used. CT slice thickness of 0.6 mm has been used. Among all the data acquired for each patient, the best systole image is individuated and imported in Mimics 21.0 (Materialise, Leuven, BE) for image segmentation. This choice allows the acquisition of the LAA in its most expanded state, with its structures made more visible in the CT images, hence easing subsequent phases.

2.2 Segmentation

The CT images do not usually allow the direct segmentation of the LAA walls due to their small difference in Hounsfield Units values with respect to the adjacent tissues. In other words, the CT contrast allows for a clear identification of the internal LAA surface, but its external surface cannot be uniquely identified. Moreover, due to the limited thicknesses in some areas, the actual patient LAA wall might result challenging to print in the desired material with the current AM technologies. Therefore, a strategy to obtain a controlled thickness simulacrum of the LAA is used, aiming for high fidelity in the reconstruction of the inner atrial surface, of the ostium, of the landing zone for the occlusion devices. At the same time, due to the aforementioned constraints, an accurate reconstruction of the real patient atrial wall thickness is neglected.

First, the LAA blood pool is isolated, using a Hounsfield threshold approach, obtaining the segmentation mask A (Figure 3 and Figure 4, pan A, in yellow); threshold values depend on the CT grey levels, which vary from patient to patient due to differences in X-rays attenuation. Experience suggests a first attempt for the threshold value around 170HU; due to the subjectiveness of the CT values from patient to patient, slightly higher or lower values might be used. This first segmentation is applied only within the LA region, avoiding the selection of voxels belonging to other cardiac chambers to reduce the noise of the generated mask.

Then a two-voxel isotropic offset of A is performed, obtaining a new segmentation mask, named B1 (Figures 3 and 4 pan B1, in green). A third segmentation mask B2 (Figures 3 and 4 pan B2, in cyan) of the blood pool is then obtained by lowering the minimum threshold value set in mask A, trying to obtain a mask

Figure 3 Segmentation masks examples

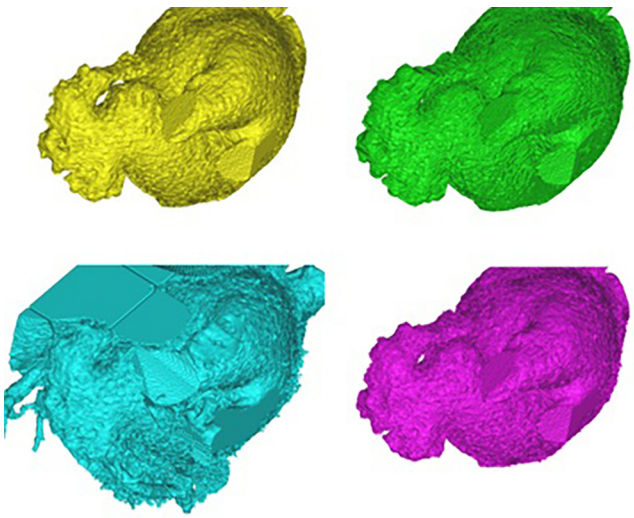

Source: Figure by authors

Figure 4 Segmentation masks

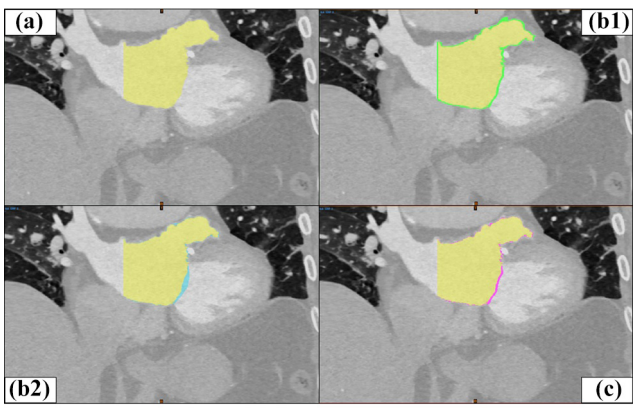

Source: Figure by authors

that defines the external LAA surface. The B2 mask is hence obtained by performing a threshold operation with HU values that do not directly correlate with the contrasted volumes highlighted by the CT. This threshold values are usually around 20% less than mask A threshold value. As a result, a higher noise level is observed in mask B2 with respect to mask A.

To de-noise the B2 mask from most of the unwanted voxels that were selected, a Boolean intersection with mask B1 is performed, creating mask C (Figures 3 and 4 pan C, in magenta). Mask A describes the internal surface of the LAA, while mask C will be processed in the following steps to obtain a functional external LAA shape. All the anatomical structures except the atrial appendage (e.g. the coronary vessels) are manually removed from A and C masks, which are then converted from a voxel map into a triangular surface mesh representation. Finally, separated wrap and global smoothing operations are performed.

2.3 3 D modeling

The A and C segmentation masks are exported in STL binary file format from Mimics and imported in Geomagic Design X (3 D Systems, Rock Hill, SC). Initial preprocessing operations are performed on the meshes, including checks for tunnels, free edges elimination and cuspid smoothing; as a result, the closed, not self-intersecting mesh of Figure 5 (left-hand pan) is produced. The mesh obtained from mask C is offset by 0.75 mm, and then a Boolean cut with mask A is performed (Figure 5, central pan, respectively in purple and cyan), obtaining the simulacrum mesh of the LA wall. The value of 0.75 mm was obtained through a trial-and-error approach in a preliminary phase of the study when different thicknesses and materials considered for the procedure were tested under the supervision of cardiac surgeons from the SHS team of the Careggi Hospital. The obtained value, combined with the adopted printing technology, provides an acceptable tradeoff between the haptic response of the model and the printability issues for thin shell structures (e.g.: print collapse due to its own weight, laceration during model manipulation). Finally, the mesh is cut using a screen polyline proximal to the appendage neck, isolating the LA appendage (Figure 5, right-hand pan), guaranteeing that the area of interest for positioning the occluding device is not removed from the mesh.

As a final check, the STL mesh of the appendage is imported back into Mimics and overlapped with the CT scans to ensure that no significant, unintended changes to the shape of the LAA inner surface occurred.

2.4 3 D printing

PreForm, a proprietary FormLabs printing software, is used as a 3 D printing preprocessing tool. Given the complex shape of the appendage model, supports are necessary for a successful

Figure 5 DesignX operations

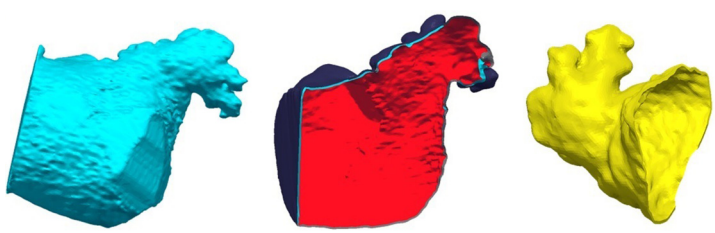

Source: Figure by authors

print. However, software automatic support generation creates an excessively dense lattice, with significant difficulties in model clean-up operations. A different strategy is applied to support generation: manual generation is used, supervised by PreForm semi-automatic checks for unsupported areas.

The manual procedure for support generation can be divided in the following steps. First of all, automatic support generation from Preform is performed. This guarantees a solid, repeatable starting point for the procedure. The manual remotion of redounding support is carried out, removing supports in each area of the model until the unsupported area warning message is displayed by the software. At this point the last removed support point is re-added.

As a result, the model clean-up procedures are simplified and undesired ruptures in the model thin wall during support removal are avoided. Figure 6 highlights the different outcome between the automatic support generation procedure proposed by PreForm (on the left-hand side) and the manual operation (right-hand side). According to the experience developed, the suggested support dimension is 0.45 mm at the contact points and internal supports should be avoided unless strictly necessary or minimized; to this purpose model orientation in the building area is suggested to be similar to the one shown in Figure 6. Concerning the layer thickness, the 0.100 mm value suggested by the software for the specific material was considered adequate.

The models are printed using a FormLabs 3B+ SLA machine in transparent Elastic 50 A material. The print process takes an average of 6.5 h for each model with an average volume of 12.8 ml of material per model. The printer allows printing up to four different models at the same time, reducing the overall total print time to about 9 h.

Once the print is completed, postprocessing operations are necessary to obtain the final usable model. First, the model is washed repetitively in tripropylene glycol monomethyl ether and soaped water to cleanse the nonpolymerized resin residuals from the solid structure. Then the model is cured in a UV oven at 60°C for 20 min, as suggested by the producer material specifications. Finally, print supports are removed using surgical forceps and pliers. Supports removal could be performed on the uncured model guarantying a better outer texture, but trial and error experience suggests the fulfillment of this critical operation after the cure, since the improved material mechanical properties due to complete polymerization help to avoid undesired lacerations or ruptures of the model thin walls.

The finished model after the print–postprocessing operations is depicted in Figure 7.

Figure 6 Preprocessing in PreForm

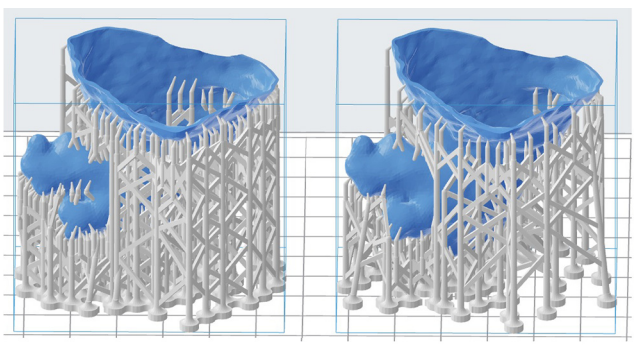

Source: Figure by authors

3. Results

The whole workflow from CT data segmentation beginning to 3 D-printed model delivery to the SHS equip requires an average of 12 h for each model; patient-specific anatomy may slightly extend the segmentation and postprocessing critical phase, but the resulting times for the global workflow are considered compatible with the hospital LAAO planning procedure time. The models were used to support the LAAO procedure in 10 different cases, assisting in the occlusion device selection and in the landing zone determination. For each patient, FE-OPS software (FEops nv, Gent, BE) provided an expert physician insight on the occlusion device sizing and landing zone; then the selected device was tested on the corresponding printed model. Out of 10 cases, the devices proposed by the software and the corresponding 3 D-printed model showed dimensional agreement on the device size and positioning in each case. Examples of the Amplatzer Amulet and of the Watchmen FLX devices positioned into the 3 D-printed models are shown in Figures 8 and 9.

4. Discussion

The workflow presented in this article was developed at the "Custom3D" laboratory (Customized 3 D in Medicine), a laboratory which supports the Careggi Hospital of

Figure 7 Left atrial appendage model

Source: Figure by authors

Figure 8 Amplatzer Amulet device positioning on 3D-printed model

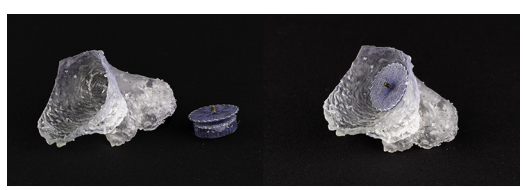

Source: Figure by authors

Figure 9 Watchmen FLX positioning on 3D-printed model

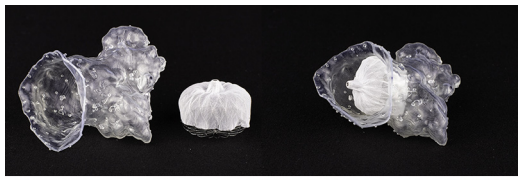

Source: Figure by authors

Florence with engineering support from the DIEF – Department of Industrial Engineering of Florence. A similar structure requires a significant economic and technical commitment and a strong cooperation between physicians and engineer. The knowledge transfer of the experience developed in this contest described in this article should be regarded as the contribution of the work to the present state of the art.

The advantages of 3 D printed models in the planning of SHS procedures, and specifically of LAAO interventions, are already acknowledged in dedicated medical literature (Bartel *et al.*, 2018; DeCampos *et al.*, 2022; Fan *et al.*, 2019; Oliveira-Santos *et al.*, 2019; Wang *et al.*, 2018). The present work does not investigate further in these benefits, but is meant to describe how to create 3 D printed models fit for the purpose.

At the moment 3 D printed models are not the tool used for the LAA occlusion device sizing at the Careggi Hospital of Florence, which still relies on the use of commercial software FE-OPS and physician expertise. On the other hand, the 3 D models created following the procedure described were used and appreciated by the medical equip to improve the understanding of patient anatomy, especially in difficult cases like retroverted or bi/trilobed LAA, and the positioning of the device in the landing zone.

In detail, the medical equip was satisfied with the haptic feedback of the material, considered suitable to represent the LAA tissue behavior. The flexibility of the model was hence deemed useful to simulate the actual positioning of the device in the LAA neck and ostium. The transparency of the model was considered helpful in the visualization of the spatial position of the device and its spatial proportion with the surrounding anatomical structures.

The next steps of the work are meant to improve the 3 D-printed model contribution in the device selection and the prediction of its mechanical interaction with the patient's atrial walls. In particular, the LAA model and device respective deformation will be studied and compared to one produced by the same device *in vivo* on the corresponding patient. Device compression is connected to LAA tissue stress and occlusion leakage, and therefore is one of the main parameters in the device selection. To this scope, 3 D printing flexible materials will be further investigated, with a particular interest in off-the-shelf and tailored tissue-mimicking polymers. A systematic evaluation of the impact of the 3 D-printed models on the clinical outcomes of the LAAO interventions will hence be addressed.

References

Al-Saady, N.M., Obel, O.A. and Camm, A.J. (1999), "Left atrial appendage: structure, function, and role in Thromboembolism", *Heart*, Vol. 82 No. 5, doi: 10.1136/hrt.82.5.547.

Aminian, A., Lalmand, J., Ben Yedder, M. and Lempereur, M. (2018), "Suboptimal device implantation may increase the occurrence of device thrombosis after left atrial appendage occlusion", *Journal of the American College of Cardiology*, Vol. 72 No. 4, doi: 10.1016/j.jacc.2018.04.076.

Bartel, T., Rivard, A., Jimenez, A., Mestres, C.A. and Müller, S. (2018), "Medical three-dimensional printing opens up new opportunities in cardiology and cardiac surgery", *European Heart Journal*, Vol. 39 No. 15, doi: 10.1093/eurheartj/ehx016.

Beigel, R., Wunderlich, N.C., Ho, S.Y., Arsanjani, R. and Siegel, R.J. (2014), "The left atrial appendage: anatomy, function, and noninvasive evaluation", *JACC: Cardiovascular Imaging*, Vol. 7 No. 12, doi: 10.1016/j.jcmg.2014.08.009.

Benjamin, E.J., Wolf, P.A., D'Agostino, R.B., Silbershatz, H., Kannel, W.B. and Levy, D. (1998), "Impact of atrial fibrillation on the risk of death: the Framingham heart study", *Circulation*, Vol. 98 No. 10, doi: 10.1161/01.CIR.98.10.946.

Blackshear, J.L. and Odell, J.A. (1996), "Appendage obliteration to reduce stroke in cardiac surgical patients with atrial fibrillation", *The Annals of Thoracic Surgery*, Vol. 61 No. 2, doi: 10.1016/0003-4975(95)00887-X.

Caliskan, E., Cox, J.L., Holmes, D.R., Meier, B., Lakkireddy, D.R., Falk, V., Salzberg, S.P. and Emmert, M. (2017), "Interventional and surgical occlusion of the left atrial appendage", *Nature Reviews Cardiology*, Vol. 14 No. 12, doi: 10.1038/nrcardio.2017.107.

Conti, M., Marconi, S., Muscogiuri, G., Guglielmo, M., Baggiano, A., Italiano, G., Mancini, M.E., Auricchio, F., Andreini, D., Rabbat, M., Guaricci, A., Fassini, G., Gasperetti, A., Costa, F., Tondo, C., Maltagliati, A., Pepi, M. and Pontone, G. (2019), "Left atrial appendage closure guided by 3D computed tomography printing technology: a case control study", *Journal of Cardiovascular Computed Tomography*, Vol. 13 No. 6, doi: 10.1016/j.jcct.2018.10.024.

de Backer, O., Arnous, S., Ihlemann, N., Vejlstrup, N., Jørgensen, E., Pehrson, S., Krieger, T.D.W., Meier, P., Søndergaard, L. and Franzen, O. (2014), "Percutaneous left atrial appendage occlusion for stroke prevention in atrial fibrillation: an update", *Open Heart*, Vol. 1 No. 1, doi: 10.1136/openhrt-2013-000020.

DeCampos, D., Teixeira, R., Saleiro, C., Oliveira-Santos, M., Paiva, L., Costa, M., Botelho, A. and Gonçalves, L. (2022), "3D printing for left atrial appendage closure: a meta-analysis and systematic review", *International Journal of Cardiology*, Vol. 356, doi: 10.1016/j.ijcard.2022.03.042.

di Biase, L., Santangeli, P., Anselmino, M., Mohanty, P., Salvetti, I., Gili, S., Horton, R., Sanchez, J., Bai, R., Mohanty, S., Pump, A., Brantes, M., Gallinghouse, G., Burkhardt, J., Cesarani, F., Scaglione, M., Natale, A. and Gaita, F. (2012), "Does the left atrial appendage morphology correlate with the risk of stroke in patients with atrial fibrillation? Results from a multicenter study", *Journal*

of the American College of Cardiology, Vol. 60 No. 6, doi: 10.1016/j.jacc.2012.04.032.

Fan, Y., Yang, F., Cheung, G.S.H., Chan, A.K.Y., Wang, D.D., Lam, Y.Y., Chow, M.C.K., Leong, M.C.W., Kam, K. H.K, So, K.C.Y., Tse, G., Qiao, Z., He, B., Kwok, K.W. and Lee, A.P.W. (2019), "Device sizing guided by Echocardiography-based three-dimensional printing is associated with superior outcome after percutaneous left atrial appendage occlusion", *Journal of the American Society of Echocardiography*, Vol. 32 No. 6, doi: 10.1016/j.echo.2019.02.003.

Furberg, C.D., Psaty, B.M., Manolio, T.A., Gardin, J.M., Smith, V.E. and Rautaharju, P.M. (1994), "Prevalence of atrial fibrillation in elderly subjects (the cardiovascular health study)", *The American Journal of Cardiology*, Vol. 74 No. 3, doi: 10.1016/0002-9149(94)90363-8.

Graf, E.C., Roppenecker, D.B., Tiemann, K., Samper, V.D. and Lueth, T.C. (2014), "Development of an anatomic heart model for the minimally-invasive closure of the left atrial appendage", *2014 IEEE International Conference on Robotics and Biomimetics, IEEE ROBIO 2014*, doi: 10.1109/ROBIO.2014.7090397.

Hachulla, A.L., Noble, S., Guglielmi, G., Agulleiro, D., Müller, H. and Vallée, J.P. (2019), "3D-printed heart model to guide LAA closure: useful in clinical practice?", *European Radiology*, Vol. 29 No. 1, doi: 10.1007/s00330-018-5569-x.

Hindricks, G., Potpara, T., Dagres, N., Arbelo, E., Bax, J.J., Blomström-Lundqvist, C., Boriani, G., Castella, M., Dan, G.A., Dilaveris, P., Fauchier, L., Filippatos, G., Kalman, J., La Meir, M., Lane, D. and Lebeau, J.P. (2021), "2020 ESC guidelines for the diagnosis and management of atrial fibrillation developed in collaboration with the European association for Cardio-Thoracic surgery (EACTS)", *Russian Journal of Cardiology*, Vol. 26 No. 9, doi: 10.15829/1560-4071-2021-4701.

Iriart, X., Ciobotaru, V., Martin, C., Cochet, H., Jalal, Z., Thambo, J.B. and Quessard, A. (2018), "Role of cardiac imaging and three-dimensional printing in percutaneous appendage closure", *Archives of Cardiovascular Diseases*, Vol. 111 Nos 6/7, doi: 10.1016/j.acvd.2018.04.005.

Kodani, E. and Akao, M. (2020), "Atrial fibrillation and stroke prevention: state of the art-epidemiology and pathophysiology: new risk factors, concepts and controversies", *European Heart Journal, Supplement*, Vol. 22, doi: 10.1093/EURHEARTJ/SUAA176.

Korsholm, K., Berti, S., Iriart, X., Saw, J., Wang, D.D., Cochet, H., Chow, D., Clemente, A., de Backer, O., Jensen, J. and Nielsen-Kudsk, J. (2020), "Expert recommendations on cardiac computed tomography for planning transcatheter left atrial appendage occlusion", *JACC: Cardiovascular Interventions*, Vol. 13 No. 3, doi: 10.1016/j.jcin.2019.08.054.

Krijthe, B.P., Kunst, A., Benjamin, E.J., Lip, G.Y.H., Franco, O.H., Hofman, A., Witteman, J.C.M., Stricker, B. and Heeringa, J. (2013), "Projections on the number of individuals with atrial fibrillation in the European union, from 2000 to 2060", *European Heart Journal*, Vol. 34 No. 35, doi: 10.1093/eurheartj/eht280.

Lee, E., Choi, E.K., Han, K. D., Lee, H.J., Choe, W.S., Lee, S. R., Cha, M.J., Lim, W.H., Kim, Y.J. and Oh, S. (2018), "Mortality and causes of death in patients with atrial fibrillation: a nationwide population-based study", *Plos One*, Vol. 13 No. 12, doi: 10.1371/journal.pone.0209687.

Nucifora, G., Faletra, F.F., Regoli, F., Pasotti, E., Pedrazzini, G., Moccetti, T. and Auricchio, A. (2011), "Evaluation of the left atrial appendage with real-time 3-dimensional transesophageal echocardiography implications for catheter-based left atrial appendage closure", *Circulation: Cardiovascular Imaging*, Vol. 4 No. 5, doi: 10.1161/CIRCIMAGING.111.963892.

Obasare, E., Mainigi, S.K., Morris, D.L., Slipczuk, L., Goykhman, I., Friend, E., Ziccardi, M.R. and Pressman, G. (2018), "CT based 3D printing is superior to transesophageal echocardiography for pre-procedure planning in left atrial appendage device closure", *The International Journal of Cardiovascular Imaging*, Vol. 34 No. 5, doi: 10.1007/s10554-017-1289-6.

Oliveira-Santos, M., de Oliveira-Santos, E., Gonçalves, L. and Silva Marques, J. (2019), "Cardiovascular three-dimensional printing in non-congenital percutaneous interventions", *Heart Lung and Circulation*, Vol. 28 No. 10, doi: 10.1016/j.hlc.2019.04.020.

Otton, J.M., Spina, R., Sulas, R., Subbiah, R.N., Jacobs, N., Muller, D.W.M. and Gunalingam, B. (2015), "Left atrial appendage closure guided by personalized 3D-printed cardiac reconstruction", *JACC: Cardiovascular Interventions*, Vol. 8 No. 7, doi: 10.1016/j.jcin.2015.03.015.

Piccini, J.P., Hammill, B.G., Sinner, M.F., Jensen, P.N., Hernandez, A.F., Heckbert, S.R., Benjamin, E.J. and Curtis, L. (2012), "Incidence and prevalence of atrial fibrillation and associated mortality among medicare beneficiaries: 1993-2007", *Circulation: Cardiovascular Quality and Outcomes*, Vol. 5 No. 1, doi: 10.1161/CIRCOUTCOMES.111.962688.

Reddy, V.Y., Gibson, D.N., Kar, S., O'Neill, W., Doshi, S.K., Horton, R.P., Buchbinder, M., Gordon, N. and Holmes, D. (2017), "Post-Approval U.S. Experience with left atrial appendage closure for stroke prevention in atrial fibrillation", *Journal of the American College of Cardiology*, Vol. 69 No. 3, doi: 10.1016/j.jacc.2016.10.010.

Ryder, K.M. and Benjamin, E.J. (1999), "Epidemiology and significance of atrial fibrillation", *The American Journal of Cardiology*, Vol. 84 No. 9, doi: 10.1016/S0002-9149(99)00713-4.

Sawaya, F.J., Chow, D.H.F., Millan-Iturbe, O. and de Backer, O. (2017), "Device-related thrombus formation with the Amplatzer Amulet LAA device: optimal implantation = optimal results", *JACC: Clinical Electrophysiology*, Vol. 3 No. 2, doi: 10.1016/j.jacep.2016.11.006.

Stoddard, M.F., Dawkins, P.R., Prince, C.R. and Ammash, N.M. (1995), "Left atrial appendage thrombus is not uncommon in patients with acute atrial fibrillation and a recent embolic event: a transesophageal Echocardiographicstudy", *Journal of the American College of Cardiology*, Vol. 25 No. 2, doi: 10.1016/0735-1097(94)00396-8.

Su, P., McCarthy, K.P. and Ho, S.Y. (2008), "Occluding the left atrial appendage: anatomical considerations", *Heart*, Vol. 94 No. 9, doi: 10.1136/hrt.2006.111989.

Unsworth, B., Sutaria, N., Davies, D.W. and Kanagaratnam, P. (2011), "Successful placement of left atrial appendage

closure device is heavily dependent on 3-dimensional transesophageal imaging", *Journal of the American College of Cardiology*, Vol. 58 No. 12, doi: 10.1016/j.jacc.2010.11.089.

Wang, Y., di Biase, L., Horton, R.P., Nguyen, T., Morhanty, P. and Natale, A. (2010), "Left atrial appendage studied by computed tomography to help planning for appendage closure device placement", *Journal of Cardiovascular Electrophysiology*, Vol. 21 No. 9, doi: 10.1111/j.1540-8167.2010.01814.x.

Wang, D.D., Gheewala, N., Shah, R., Levin, D., Myers, E., Rollet, M. and O'Neill, W.W. (2018), "Three-dimensional printing for planning of structural heart interventions", *Interventional Cardiology Clinics*, Vol. 7 No. 3, doi: 10.1016/j.iccl.2018.04.004.

Wilke, T., Groth, A., Mueller, S., Pfannkuche, M., Verheyen, F., Linder, R., Maywald, U., Bauersachs, R. and Breithardt, G. (2013), "Incidence and prevalence of atrial fibrillation: an analysis based on 8.3 million patients", *Europace*, Vol. 15 No. 4, doi: 10.1093/europace/eus333.

Corresponding author

Tommaso Stomaci can be contacted at: tommaso.stomaci@unifi.it